frontiers | Frontiers in Materials

TYPE Original Research
PUBLISHED 08 August 2024
DOI 10.3389/fmats.2024.1436577

OPEN ACCESS

EDITED BY
Li Li,
Peking University, China

REVIEWED BY
Fusheng Tan,
Tsinghua University, China
Zhu Changjun,
Central South University, China
Fang Li,
Central South University, in collaboration with reviewer ZC

*CORRESPONDENCE
Jing Peng,
jingpeng@hnu.edu.cn
Hui Feng,
fenghuiff@hnu.edu.cn

RECEIVED 22 May 2024
ACCEPTED 23 July 2024
PUBLISHED 08 August 2024

CITATION
Song J, Zhang J, Peng J, Song X, Liang L and Feng H (2024) Mechanical properties and deformation behavior of a high entropy alloy with precipitate under cycle loading. *Front. Mater.* 11:1436577. doi: 10.3389/fmats.2024.1436577

Mechanical properties and deformation behavior of a high entropy alloy with precipitate under cycle loading

Junhan Song[1], Jie Zhang[1], Jing Peng[2]*, Xinhua Song[3], Long Liang[1] and Hui Feng[2]*

[1]Changsha Institute of Mining Research Co., Ltd., Changsha, China, [2]College of Mechanical and Vehicle Engineering, Hunan University, Changsha, China, [3]Zhangjiajie Aviation Industry Vocation Technical College, Zhangjiajie, China

Compared to the traditional alloys, high entropy alloys exhibit exceptional strength and outstanding ductility, making them highly attractive for use in demanding engineering applications. However, the atomic-scale deformation behavior of HEAs with precipitate under the low-cycle loading conditions has not been well studied. Here, we utilize molecular dynamics simulations to investigate the low cycle fatigue behavior of AlCoCrFeNi HEAs with AlNi-rich phase, in order to better understand the cyclic deformation, work hardening, and damage mechanisms. In the stress-strain hysteresis loops, the stress in the elastic stage exhibits a gradual linear increase, followed by fluctuations at yielding and plastic deformation. The strain hardening depends on the cycle number after the yielding stage. With an increase in the number of cycles, the activation mode of stacking faults gradually transitions from a multi-slip system to a single-slip system, attributed to the gradual phase transformation. A thorough examination of dislocation evolution is crucial in understanding the strengthening and plastic behavior of materials under cyclic loading. The generation of more stair-rod dislocations further suppresses the movement of dislocations. The combined effects of element diffusion, structural transformation, and incoherent precipitation play a critical role in enhancing the mechanical properties of AlCoCrFeNi HEAs. The strength of high entropy alloys is improved through interface strengthening caused by element diffusion and structural transformation, along with dispersion induced by incoherent precipitation. This work provides a detailed atomic-level understanding of the cyclic deformation-induced strengthening mechanism, in order to design high-strength and ductile HEAs with specific desired properties.

KEYWORDS

high entropy alloys, low cycle fatigue, deformation behaviour, precipitation, mechanical property

1 Introduction

Distinct from the conventional alloy, high entropy alloys (HEA) with the characteristic of multi-principal elements have attracted widespread attention for their outstanding properties, such as high strength (Lei et al., 2018; Yan et al., 2022), high corrosion resistance (Nene et al., 2019; Luo et al., 2020), and superior resistance to wear (Yang et al., 2022;

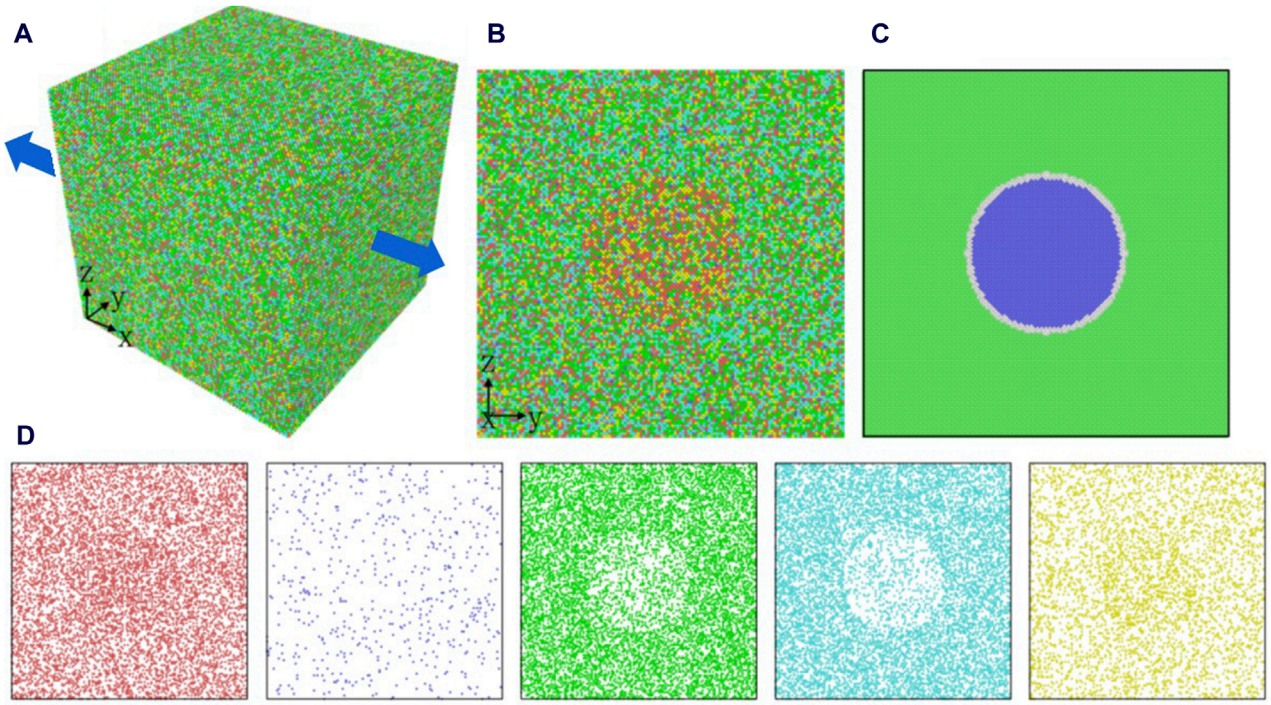

FIGURE 1
Atomic model of AlCoCrFeNi HEA, which is colored according to the atom type **(A)**. Al, Co, Cr, Fe, and Ni. Element distribution of AlNi-rich phase in HEA **(B)**. The corresponding microstructure based on the CNA value **(C)**. BCC, FCC, and other. The distribution of Al, Co, Cr, Fe, and Ni element **(D)**.

TABLE 1 Computational parameters used in the MD simulations.

Material	AlCoCrFeNi HEA	AlNi-rich phase
Composition	Al 11.8, Co 19.1, Cr 4.4, Fe 34.7, Ni 30.0 (at%)	Al 23.1, Co 16.0, Cr 2.3, Fe 23.4, Ni 35.3 (at%)
Phase	FCC	BCC
Lattice parameter	3.622 Å	2.877 Å
Dimension	$25.3 \times 25.3 \times 25.3\ nm^3$	5.4 nm
Atomic count	1,315,595	56,449
Time step	1 fs	
Temperature	300 K	
Strain rate	$1 \times 10^8\ s^{-1}$	

Wang et al., 2024). These alloys exhibit extensive application prospect in some key fields such as aerospace, nuclear industry and transportation attributed to their unique structure and the remarkable performance (Kaushik et al., 2022; Li F. et al., 2024). However, higher demands are placed on the fatigue performance of alloys in long-term service environments. It is essential to thoroughly examine and uncover the evolution process of microstructures, such as grain structure and second-phase particles, as well as their influence on performance during cyclic deformation. This investigation is crucial for enhancing fatigue performance through the implementation of microstructure design strategies.

Recently, considerable research efforts have been dedicated to developing HEAs with improved fatigue resistance and investigating the mechanisms underlying their fatigue resistance (Li W. et al., 2020; Picak et al., 2021; Hu et al., 2024). For example, by studying the low cycle fatigue behavior of the CoCrFeMnNi HEA with two different grain sizes, it is found that the fatigue life and hardening behavior are determined by refined grain size, high-density dislocation walls, and the annihilation of existing dislocations

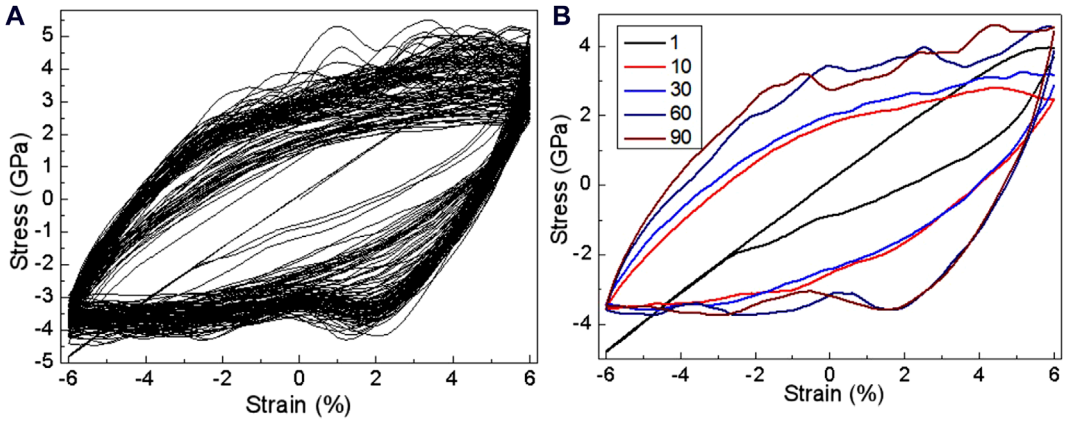

FIGURE 2
(A) Cyclic stress-strain curves with the increasing cycles. **(B)** The cyclic stress-strain curves for 1st, 10th, 30th, 60th, and 90th cycles.

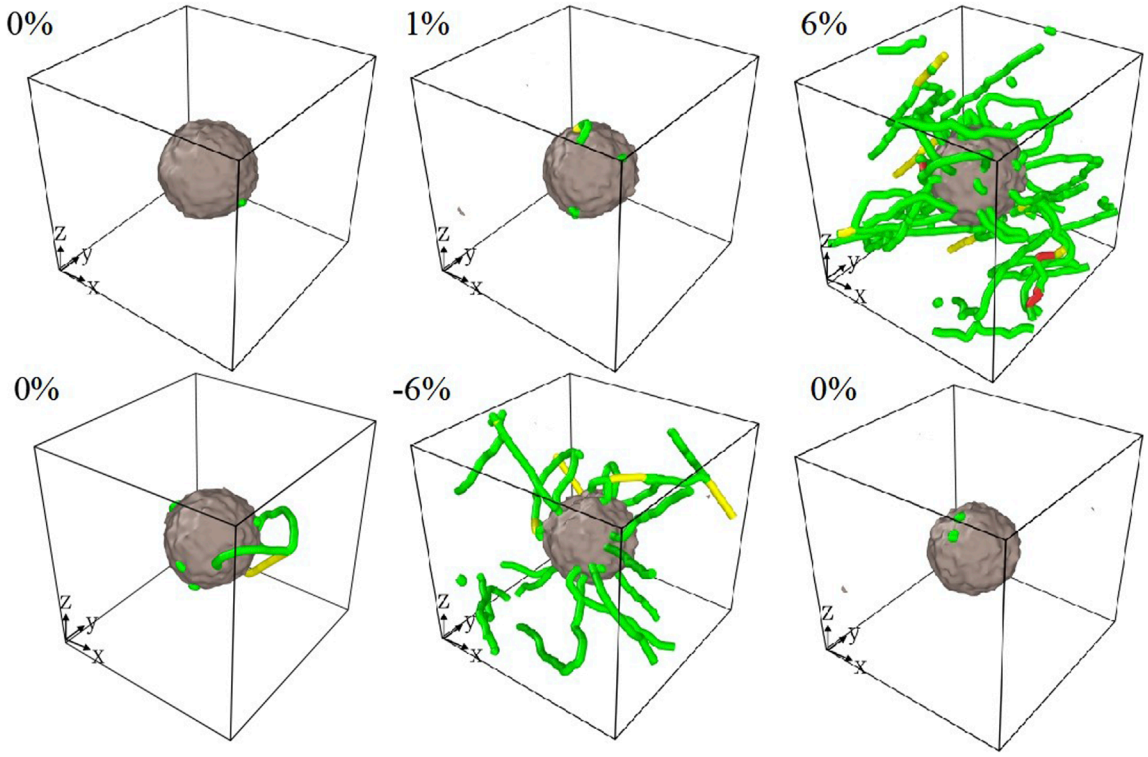

FIGURE 3
The microstructures for dislocation interacting with AlNi-rich phase in the first cycle loading at the strain: 0, 1%, 6%, 0%, −6%, and 0%. Here, the 1/6 < 112> (green line),1/6 <100> (pink line), 1/2 < 111> <110> (blue line), 1/3 <001> (yellow line), 1/3 < 111> (sky blue line), and other (red line) dislocations.

(Lu et al., 2021; Picak et al., 2021). In addition, the deformation twinning plays a crucial role in high cycle fatigue process of CoCrFeMnNi HEA. The formation of deformation twinning enhances the yield strength and working hardening behavior of this HEA, but the presence of a large amount of deformation twinning can generate micro voids, thereby acceleration the initiation and propagation of cracks (Kim et al., 2019). Compared to traditional alloys, the formation of nanotwin in two-phase FCC Al0.5CoCrCuFeNi HEA leads to strengthening during fatigue process, providing great durability limits and crack initiation resistance (Tang et al., 2015). The difference in deformation behavior between the cyclic loading and uniaxial tension of Fe30Mn10Co10Cr0.4C HEA is compared, and it is found that the ε-martensitic hardening effect is weaker during cyclic deformation due to the planarity of slip and partial reversibility of deformation compared to that in uniaxial tension (Shams et al., 2022a).

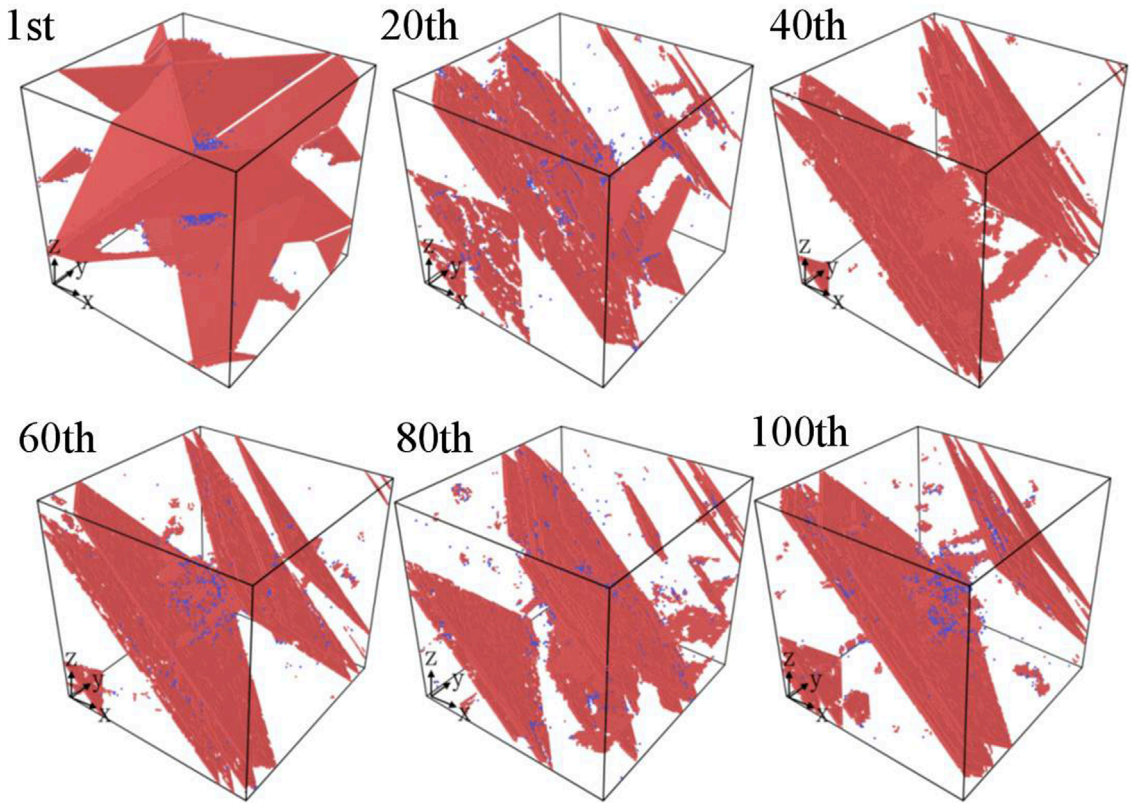

FIGURE 4
The microstructures for the cycle number: 1st, 20th, 40th, 60th, 80th, and 100th. BCC, HCP, and other.

Several studies have indicated that the martensitic transformation and ductile-to-transformable properties of multicomponent B2 precipitates in HEA have the potential to enhance resistance to fatigue crack initiation and improve fatigue performance at low strain amplitudes (Feng et al., 2021).

Based on the research mentioned, it is evident that investigating the dynamic evolution mechanism of microstructure during the cycling process is advantageous for expediting the development of fatigue-resistant HEAs. However, it is difficult to reveal the dynamic interaction of microstructure during the cyclic deformation through experiments. Thus, MD simulation method is widely used to investigate the dynamic interaction of microstructures during deformation (Li J. et al., 2020; Peng et al., 2021; Yin et al., 2021; Zhang et al., 2022; Wang Y. et al., 2023). The cyclic nanoindentation simulation is conducted using MD method. It is found that the amorphous transition occurred at different loading rates, and the rate dependence of deformation behavior increased with increasing number of cycles (Luo et al., 2024). During the cyclic deformation process of AlCrCuFeNi HEA under tension and compression, the partial dislocation interactions lead to lattice disorder, which hinders the reverse slip of dislocations and reduces the Bauschinger effect (Nguyen et al., 2023). The low cycle cycling of nanocrystalline refractory HEA with different grain sizes is simulated by MD method. The grain growth behavior during the cycling process drive the dynamic Hall-petch strengthening mechanism. As the grain size decreases, the dominant deformation mechanism changes from dislocation dominated to deformation twinning (Peng et al., 2020). By studying the cyclic loading deformation response under different strain amplitudes, the phase transition mechanism activated under high strain amplitude loading is revealed (Zhang et al., 2024). The atomic scale mechanism of unique precipitation behavior near grain boundaries under cyclic loading conditions has been studied (Li L. et al., 2024).

Taking into account the current problems, the low cycle loading of AlCoCrFeNi HEAs with precipitated phases is carried out at atomic scale in the present work. The interaction behavior between precipitates and microstructure during the cycling process is investigated, which helps to understand the work hardening and cyclic deformation mechanism under the influence of cyclic cycles and precipitates, and accelerates the design of fatigue resistant high entropy alloys.

2 Method

The cyclic loading of AlCoCrFeNi HEA is carried out using the Large-scale Atomic/Molecular Massively Parallel Simulator (LAMMPS) (Plimpton, 1995), as shown in Figure 1A. According to previous study, the as-deposited AlCoCrFeNi HEA comprises of FCC and BCC phase (Shen et al., 2021a; Shen et al., 2021b). Thus, in the present work, the structure of the HEA is characterized by the FCC phase (Shen et al., 2021a; Shen et al., 2021b), with the AlNi-rich phase exhibiting an ordered BCC phase (Figures 1B,C). The lattice parameters of the FCC and BCC phases are 3.622

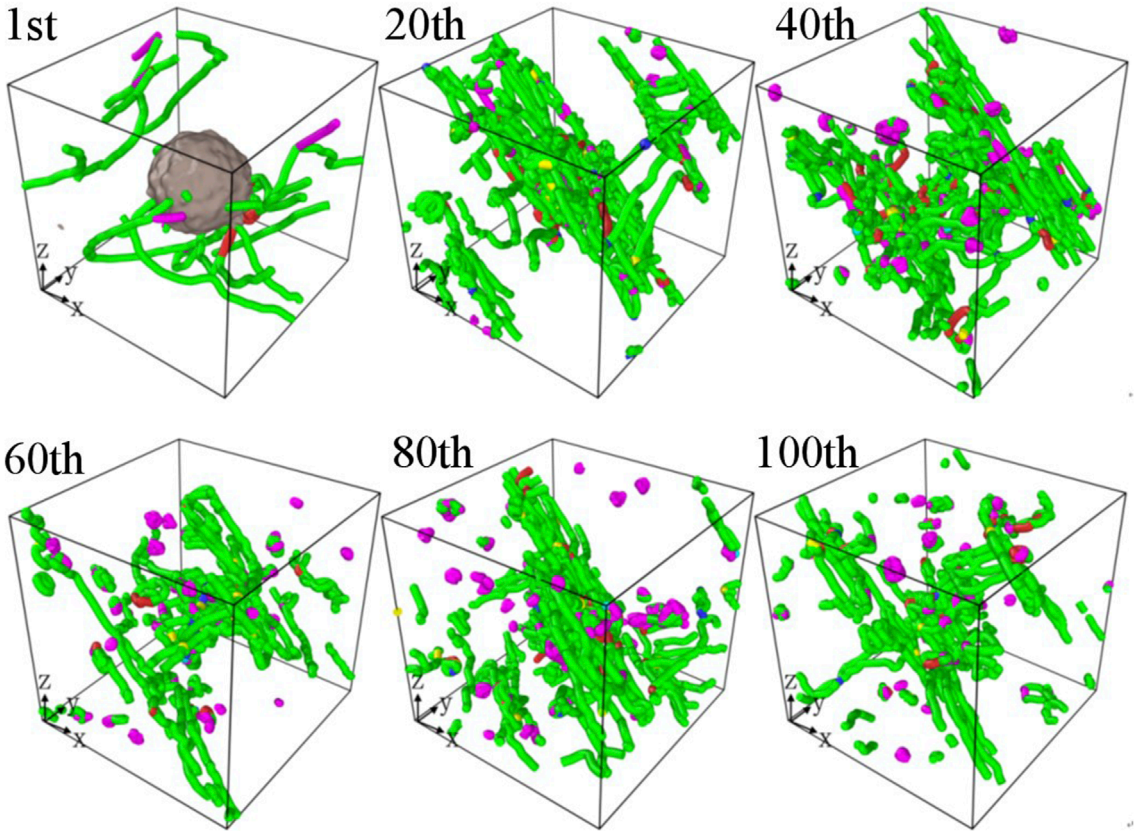

FIGURE 5
The dislocation characteristics for the cycle number: 1st, 20th, 40th, 60th, 80th, and 100th. Here, the 1/6 <112> (green line),1/6 <100> (pink line), 1/2 < 111> <110> (blue line), 1/3 <001> (yellow line), 1/3 < 111> (sky blue line), and other (red line) dislocations.

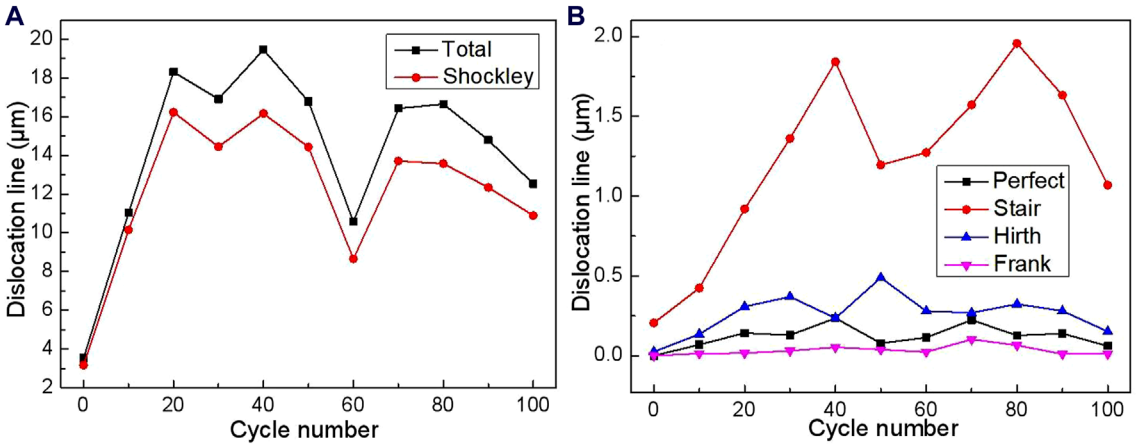

FIGURE 6
(A) The total length of dislocation line, and **(B)** the types and lengths of dislocation line for the cycle number: 0, 20, 40, 60, 80, and 100.

and 2.877 Å, respectively (Shen et al., 2021a; Shen et al., 2021b). The embedded atom method (EAM) is utilized in the analysis of the AlCoCrFeNi HEA (Farkas and Caro, 2020). The dimensions of the HEA sample are 25.3 nm × 25.3 nm × 25.3 nm, with a sphere precipitate radius of 5.4 nm. The sample consists of a total of 903,000 atoms. Figure 1D showcases the element distribution of both the matrix and precipitate phases, with each element being evenly dispersed. The specific computational parameters can be found in Table 1. The orientation of both AlCoCrFeNi HEA and AlNi-rich phase are defined by the x, y, and z directions, which correspond to [100], [010], and [001], respectively. Periodic boundary conditions are applied in all three directions (Li et al.,

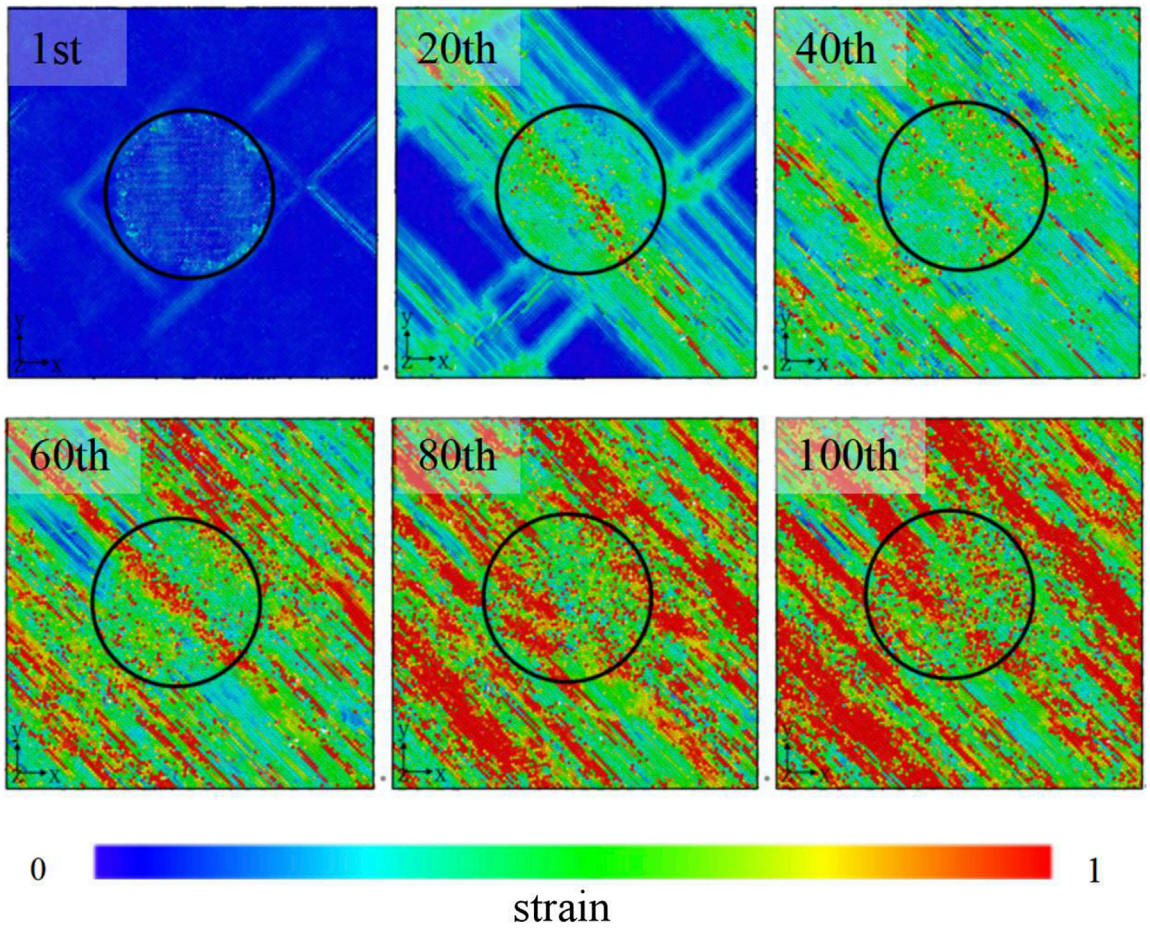

FIGURE 7
The strain distribution for the cycle number: 1st, 20th, 40th, 60th, 80th, and 100th. The red atoms refer to the high strain region while blue atoms represent the low strain region.

2018; Li J. et al., 2020; Li et al., 2022b). The deformation occurs along the x-axis at a constant rate of $1 \times 10^8\ s^{-1}$, which is widely used in previous studies (Li L. et al., 2020; Peng et al., 2021; Li et al., 2022b). Initially, the sample system is in its minimum energy state at a temperature of 300 K. The open visualization tool OVITO is utilized for post-processing the simulation data (Stukowski, 2009). The microstructures are analyzed by using common neighbor analysis (CNA) (Clarke and Jónsson, 1993), and dislocation analysis (DXA) (Stukowski et al., 2012).

3 Results and discussion

Figure 2 shows the cyclic stress-strain behavior of AlCoCrFeNi HEA as the cycle number increases. In the stress-strain hysteresis loops, the stress in the elastic stage shows a linear increase, followed by gradual fluctuations at yielding and plastic deformation up to 6% strain. This pattern is consistent with results from monotonic loading. Depending on the cycle number, strain-softening or strain-hardening can occur after the yielding stage (Juan et al., 2015; Juan et al., 2016), as depicted in Figure 2A. For the cycle numbers below 60, strain-hardening intensifies with increasing cycles, while strain-softening is observed at the yielding strain. Conversely, at low cycle numbers, strain-softening occurs initially, followed by gradual strengthening of strain-hardening at higher cycle numbers (Figure 2B). The presence of strain-hardening/softening in stress-strain curves is attributed to changes in microstructure, such as dislocation nucleation/movement and deformation twinning during cyclic loading (Lam et al., 2020; Feng et al., 2021). This cyclic stress response aligns with findings from previous studies on HEAs using both experiments and MD simulations (Picak et al., 2021; Lam et al., 2023).

The dislocation evolution within the first cycle loading is exhibited in Figure 3. When the strain increase from 0% to 6%, the dislocations first proliferate from the interface of phase during the tension stage. When the strain recovers from 6% to 0%, dislocations annihilate due to the recovery of the atom lattice. Subsequently, during the reverse loading process, dislocation proliferate again. However, the dislocation density during compression process is significantly lower than that during tensile process.

In order to investigate the strain-hardening mechanism, Figure 4 illustrates the evolution of microstructure at various cycle numbers. At a strain of 6%, a significant number of stacking faults are generated to accommodate the plastic deformation of the

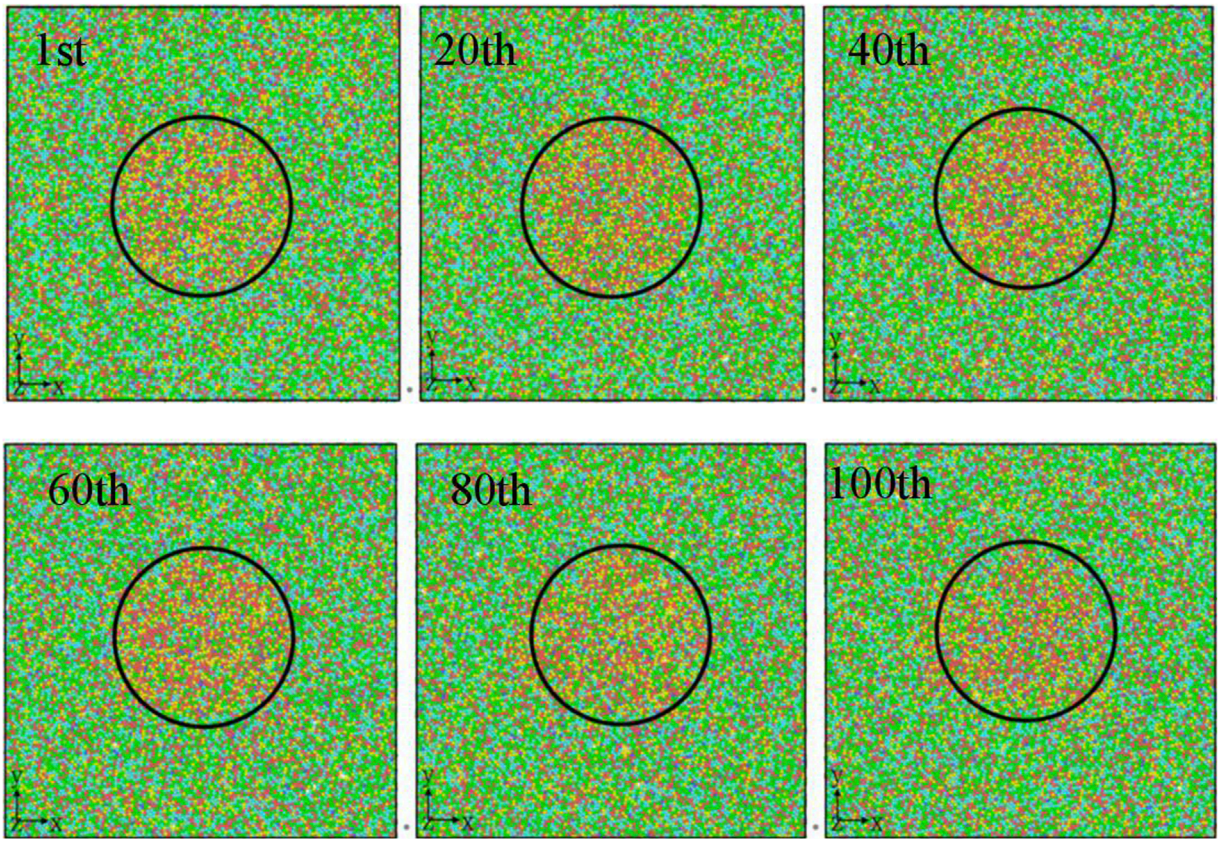

FIGURE 8
The element distribution for the cycle number: 1st, 20th, 40th, 60th, 80th, and 100th. Al, Co, Cr, Fe, and Ni.

AlCoCrFeNi HEA (Bahadur et al., 2022; Wang X. et al., 2023). It is evident that with an increase in the number of cycles, there is a marked change in the stacking fault structure. The focus remains primarily on the activation of the slip system on the <112> plane. Initially, during the cyclic loading process, stacking faults can be activated on multiple slip planes. However, as the number of cycles increases, the activation mode of stacking faults gradually shifts from a multi-slip system to a single-slip system. This shift indicates that the contribution of precipitated phases has a more pronounced effect on the plastic deformation mechanism of the material in the early stages, particularly on the slip system that facilitates the activation of stacking faults. As the number of cyclic loading increases in the later stages, the influence of precipitated phases gradually diminishes, and eventually may no longer exhibit a significant impact on the deformation mechanism. This transition is attributed to the gradual transformation of body-centered cubic (BCC) precipitates into face-centered cubic (FCC) structures induced by plastic deformation (Lu et al., 2019; Li W. et al., 2020; Lu et al., 2021). This transformation enhances interfacial cohesiveness, thereby influencing the mechanical properties of HEAs.

The behavior of dislocations is a crucial factor in determining the strength and ductility of materials (Li et al., 2023; Chen et al., 2024). Figure 5 shows the evolution of dislocation distribution with the increasing cycle number at a strain of 6%. During the early stages of cyclic loading deformation, a large number of Shockley partial dislocations form near the precipitated phase. As the number of cyclic loading increases, the precipitated phase undergoes a transformation from BCC to FCC system. This trend results in a significant amount of Shockley partial dislocations that are able to penetrate the precipitate. However, these Shockley partial dislocations gradually shift from long, straight lines to shorter lines, ultimately contributing to the plastic deformation. Simultaneously, the formation of stair-rod dislocations takes place, and the density of these dislocations increases as cyclic loading progresses. The increase of stair-rod dislocations plays a crucial role in strengthening the AlCoCrFeNi HEAs. The thorough examination of dislocation evolution is essential in understanding the strengthening and plastic behavior of materials under cyclic loading (Zou et al., 2022). This analysis is an important and crucial role in revealing the strain and hardening induced by cyclic loading.

Here, to analyse the influence of cycle number on the ductility of the HEAs, the variation of the mobile dislocation density with the increased cycle number is counted in Figure 6, where the Shockley partial dislocations are mobile. As the cycle number increases, the mobile dislocation density not only increases significantly in quantity, but also experiences a rapid rate of multiplication (Shams et al., 2022b). The more stair-rod dislocations are generated, further suppressing the movement of dislocations. Therefore, it can be inferred that the larger cycle number is advantageous for improving the ductility and strength of AlCoCrFeNi HEAs (Suzuki et al., 2020).

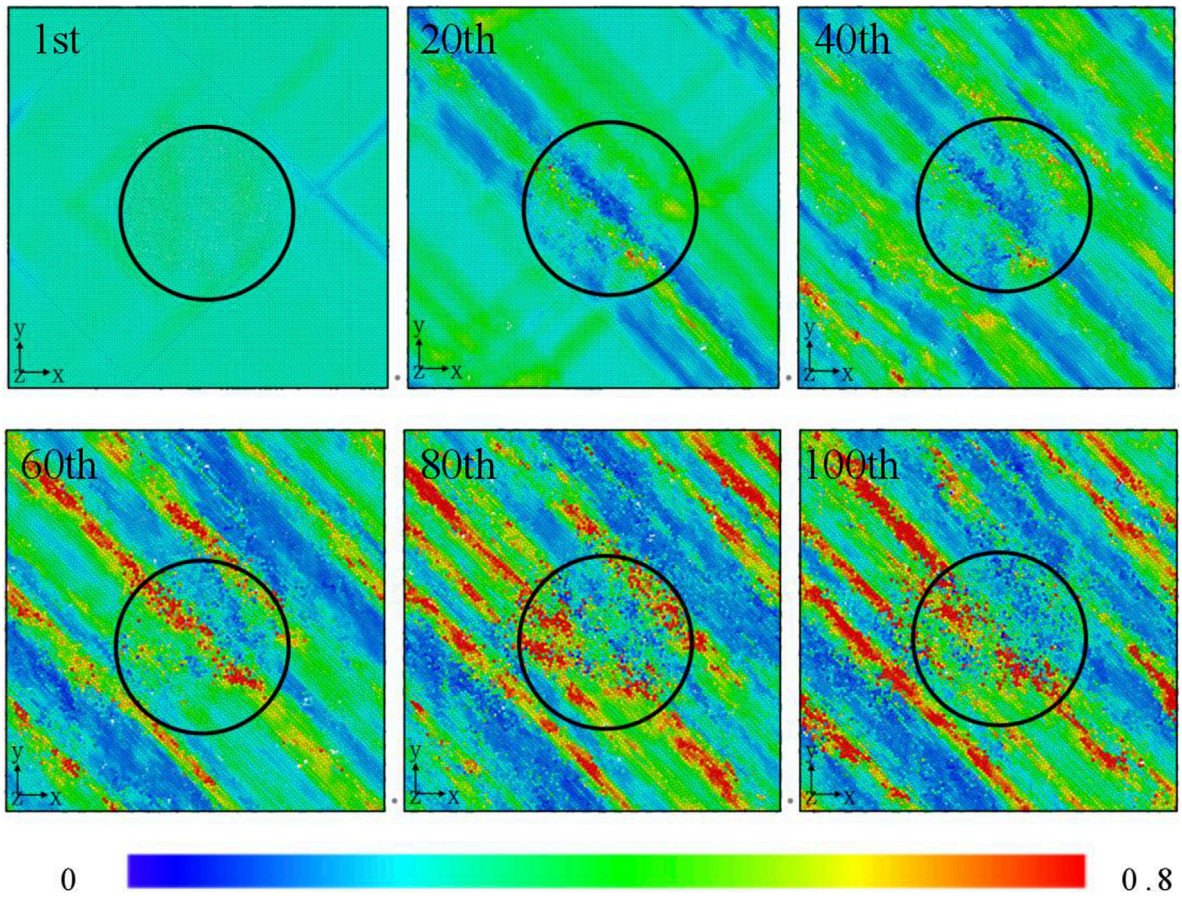

FIGURE 9
The strain gradient distribution for the cycle number: 1st, 20th, 40th, 60th, 80th, and 100th. The red atoms refer to the high deformation gradient region while blue atoms represent the low deformation gradient region.

Here, the atomic shear strain of AlCoCrFeNi HEA is investigated at various cycle numbers and under a uniaxial tension strain of 6%. The distribution of shear strain is determined by calculating the von Mises local shear invariant, with the initial configuration prior to uniaxial tension serving as the baseline (Shimizu et al., 2007). Figure 7 illustrates a lattice distortion field observed in the HEA (Li et al., 2022a), with red indicating regions of high strain and blue representing regions of zero strain. At the 1st cycle, the high strain appears there within the phase regions. As the number of cycles increases, local shear transformation zones (STZs) are formed during the plastic deformation stage (Picak et al., 2021). This is caused by the accumulation of local shear strain in the HEA. However, AlNi-rich phase suppresses the formation of shear bands at high cycle number (Figure 7). With the further increase of the cycle number, the local deformation becomes more pronounced, leading to a continued increase in shear strain that spreads throughout the AlCoCrFeNi HEA. Numerous shear bands are observed throughout the entirety of the deformation process, suggesting that the AlCoCrFeNi HEA has experienced intricate plastic deformation.

Figure 8 presents the composition evolution of an ordered AlNi-rich phase. The cyclic loading induces element diffusion within the AlNi-rich phase, leading to the transformation-induced plasticity effect (Wang et al., 2019). This phenomenon results in element segregation and phase transformation within the metastable single-phase HEA. Additionally, the fluctuations in elemental distribution caused by element diffusion may dissolve AlNi-rich nano-precipitates, ultimately enhancing strength without compromising ductility (Jiang et al., 2017). The combined effects of element diffusion, structural transformation, and incoherent precipitation play a critical role in enhancing the mechanical properties of AlCoCrFeNi HEAs. These mechanisms offer a range of possibilities for designing new alloys that offer improved strength and ductility simultaneously.

The lattice vectors for each atom are identified for both the reference and current configurations, allowing for the calculation of the deformation gradients for each individual atom. Figure 9 shows the deformation gradients at a strain of 6% for various cycle numbers. As is well known, the nucleation and movement of dislocations can significantly decrease the elastic strain. In other words, localized plastic deformation decreases the elastic strain in regions experiencing increased strain after yielding. In the low cycle number, the deformation gradient can be more clearly observed with the activation of more plastic behavior (Figure 9). The element diffusion, structural transformation, and incoherent precipitation inhibit the strain gradient. This is the microscopic root cause of strain hardening in AlCoCrFeNi HEAs on the atomic level.

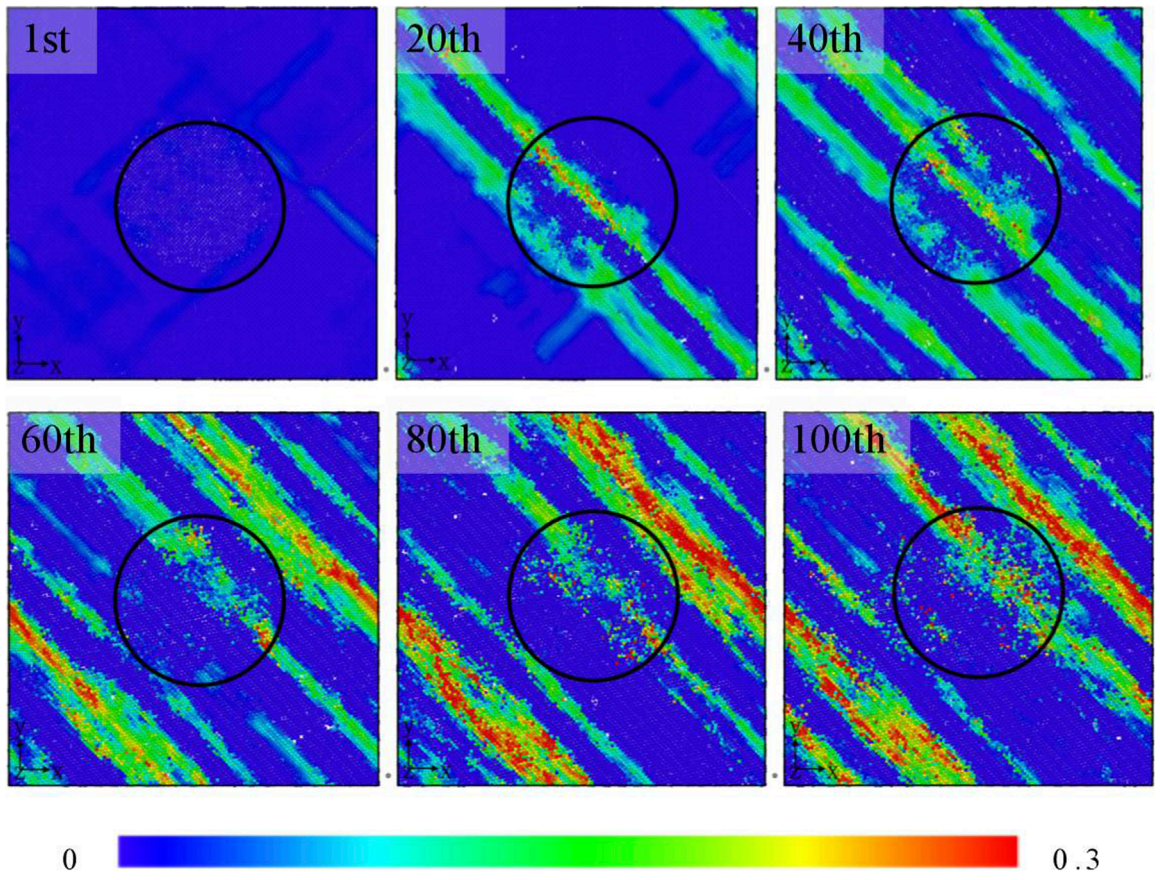

FIGURE 10
The microrotation distribution along the z direction for the cycle number: 1st, 20th, 40th, 60th, 80th, and 100th. The red atoms refer to the region of high microrotation in a clockwise direction while blue atoms represent the region of low microrotation.

The previous work demonstrates that the microrotation is not only a useful measure for determining deformation (Guo et al., 2020), but also able to capture the nanoscale deformation (e.g., dislocation slip, grain boundary sliding, and migration) (Tucker et al., 2012). Figure 10 shows the distribution of the microrotation fields along the z-axis. Atoms are color-coded based on the computed microrotation. Interestingly, certain regions display a noticeable microrotation despite the absence of high strain (see Figures 8, 9). Additionally, the microrotation patterns surrounding the ordered phase (Figure 10) closely resemble those illustrated in Figure 9. Thus, the strength of HEA is enhanced through interface strengthening caused by element diffusion and structural transformation, as well as dispersion induced by incoherent precipitation.

4 Conclusion

In present work, MD simulations have been conducted to study the microscopic cycle deformation mechanism and mechanical properties of AlxCoCrFeNi HEAs with the AlNi-rich phase, and the effects of cycle number are taken into account. In stress-strain hysteresis loops, the stress in the elastic stage shows a gradual linear increase, followed by fluctuations at yielding and plastic deformation. The degree of strain hardening is influenced by the number of cycles after yielding. As the number of cycles increases, the activation mode of stacking faults shifts from a multi-slip system to a single-slip system due to gradual phase transformation. Understanding the evolution of dislocations is essential in comprehending the strengthening and plastic behavior of materials under cyclic loading. The formation of additional stair-rod dislocations further impedes the movement of dislocations. The combined effects of element diffusion, structural transformation, and incoherent AlNi-rich precipitation significantly enhance the mechanical properties of AlCoCrFeNi HEAs. The strength of HEA is bolstered through interface strengthening from element diffusion and structural transformation, as well as dispersion induced by incoherent precipitation. The present study offers valuable insights into the nanoscale deformation mechanism of complex HEAs, and serves as a catalyst for more in-depth experimentation in microstructure design.

Data availability statement

The original contributions presented in the study are included in the article/supplementary material, further inquiries can be directed to the corresponding authors.

Author contributions

JS: Data curation, Formal Analysis, Investigation, Software, Writing–original draft. JZ: Conceptualization, Software, Writing–original draft. JP: Formal Analysis, Software, Writing–review and editing. XS: Data curation, Methodology, Validation, Writing–original draft. LL: Formal Analysis, Investigation, Methodology, Writing–original draft. HF: Conceptualization, Methodology, Validation, Writing–review and editing.

Funding

The author(s) declare that financial support was received for the research, authorship, and/or publication of this article. The authors would like to deeply appreciate the supports from the Natural Science Foundation of Changsha City (Grant No. kq2202139), the Hunan Provincial Natural Science Foundation of China (2022JJ60012) and the Key Research and Development Program sponsored by Hunan Province (2023SK 2076).

Conflict of interest

Authors JS, JZ, and LL were employed by Changsha Institute of Mining Research Co., Ltd.

The remaining authors declare that the research was conducted in the absence of any commercial or financial relationships that could be construed as a potential conflict of interest.

Publisher's note

References

Bahadur, F., Jain, R., Biswas, K., and Gurao, N. P. (2022). Low cycle fatigue behaviour of non-equiatomic TRIP dual-phase Fe50Mn30Co10Cr10 high entropy alloy. *Int. J. Fatigue* 155, 106545. doi:10.1016/j.ijfatigue.2021.106545

Chen, Y., Feng, H., Li, J., Liu, B., Jiang, C., Liu, Y., et al. (2024). Dislocation flow turbulence simultaneously enhances strength and ductility. *Proc. Natl. Acad. Sci.* 121, e2316912121. doi:10.1073/pnas.2316912121

Clarke, A. S., and Jónsson, H. (1993). Structural changes accompanying densification of random hard-sphere packings. *Phys. Rev. E* 47, 3975–3984. doi:10.1103/physreve.47.3975

Farkas, D., and Caro, A. (2020). Model interatomic potentials for Fe–Ni–Cr–Co–Al high-entropy alloys. *J. Mater. Res.* 35, 3031–3040. doi:10.1557/jmr.2020.294

Feng, R., Rao, Y., Liu, C., Xie, X., Yu, D., Chen, Y., et al. (2021). Enhancing fatigue life by ductile-transformable multicomponent B2 precipitates in a high-entropy alloy. *Nat. Commun.* 12, 3588. doi:10.1038/s41467-021-23689-6

Guo, Y., Collins, D. M., Tarleton, E., Hofmann, F., Wilkinson, A. J., and Britton, T. B. (2020). Dislocation density distribution at slip band-grain boundary intersections. *Acta Mater* 182, 172–183. doi:10.1016/j.actamat.2019.10.031

Hu, J., Yang, K., Wang, Q., Zhao, Q. C., Jiang, Y. H., and Liu, Y. J. (2024). Ultra-long life fatigue behavior of a high-entropy alloy. *Int. J. Fatigue* 178, 108013. doi:10.1016/j.ijfatigue.2023.108013

Jiang, S., Wang, H., Wu, Y., Liu, X., Chen, H., Yao, M., et al. (2017). Ultrastrong steel via minimal lattice misfit and high-density nanoprecipitation. *Nature* 544, 460–464. doi:10.1038/nature22032

Juan, C.-C., Tsai, M.-H., Tsai, C.-W., Hsu, W.-L., Lin, C.-M., Chen, S.-K., et al. (2016). Simultaneously increasing the strength and ductility of a refractory high-entropy alloy via grain refining. *Mat. Lett.* 184, 200–203. doi:10.1016/j.matlet.2016.08.060

Juan, C.-C., Tsai, M.-H., Tsai, C.-W., Lin, C.-M., Wang, W.-R., Yang, C.-C., et al. (2015). Enhanced mechanical properties of HfMoTaTiZr and HfMoNbTaTiZr refractory high-entropy alloys. *Intermetallics* 62, 76–83. doi:10.1016/j.intermet.2015.03.013

Kaushik, N., Meena, A., and Mali, H. S. (2022). High entropy alloy synthesis, characterisation, manufacturing & potential applications: a review. *Mat. Manuf. Process.* 37, 1085–1109. doi:10.1080/10426914.2021.2006223

Kim, Y.-K., Ham, G.-S., Kim, H. S., and Lee, K.-A. (2019). High-cycle fatigue and tensile deformation behaviors of coarse-grained equiatomic CoCrFeMnNi high entropy alloy and unexpected hardening behavior during cyclic loading. *Intermetallics* 111, 106486. doi:10.1016/j.intermet.2019.106486

Lam, T.-N., Chin, H.-H., Zhang, X., Feng, R., Wang, H., Chiang, C.-Y., et al. (2023). Tensile overload-induced texture effects on the fatigue resistance of a CoCrFeMnNi high-entropy alloy. *Acta Mat.* 245, 118585. doi:10.1016/j.actamat.2022.118585

Lam, T.-N., Lee, S. Y., Tsou, N.-T., Chou, H.-S., Lai, B.-H., Chang, Y.-J., et al. (2020). Enhancement of fatigue resistance by overload-induced deformation twinning in a CoCrFeMnNi high-entropy alloy. *Acta Mater* 201, 412–424. doi:10.1016/j.actamat.2020.10.016

Lei, Z., Liu, X., Wu, Y., Wang, H., Jiang, S., Wang, S., et al. (2018). Enhanced strength and ductility in a high-entropy alloy via ordered oxygen complexes. *Nature* 563, 546–550. doi:10.1038/s41586-018-0685-y

Li, F., Dong, T., Zhang, C., Chen, G., Chen, S., Chen, K., et al. (2024a). Controllable precipitation behavior near grain boundaries enabled by artificial strain concentration in age-hardening aluminum alloys. *Mat. Sci. Eng. A* 892, 146026. doi:10.1016/j.msea.2023.146026

Li, J., Chen, H., Fang, Q., Jiang, C., Liu, Y., and Liaw, P. K. (2020a). Unraveling the dislocation–precipitate interactions in high-entropy alloys. *Int. J. Plast.* 133, 102819. doi:10.1016/j.ijplas.2020.102819

Li, J., Chen, Y., He, Q., Xu, X., Wang, H., Jiang, C., et al. (2022a). Heterogeneous lattice strain strengthening in severely distorted crystalline solids. *Proc. Natl. Acad. Sci.* 119 (25), e2200607119. doi:10.1073/pnas.2200607119

Li, J., Fang, Q., Liu, B., and Liu, Y. (2018). Transformation induced softening and plasticity in high entropy alloys. *Acta Mater* 147, 35–41. doi:10.1016/j.actamat.2018.01.002

Li, J., Fu, X., Feng, H., Liu, B., Liaw, P. K., and Fang, Q. (2023). Evaluating the solid solution, local chemical ordering, and precipitation strengthening contributions in multi-principal-element alloys. *J. Alloys Compd.* 938, 168521. doi:10.1016/j.jallcom.2022.168521

Li, J., Xie, B., He, Q., Liu, B., Zeng, X., Liaw, P. K., et al. (2022b). Chemical-element-distribution-mediated deformation partitioning and its control mechanical behavior in high-entropy alloys. *J. Mat. Sci. Technol.* 120, 99–107. doi:10.1016/j.jmst.2021.11.065

Li, L., Chen, H., Fang, Q., Li, J., Liu, F., Liu, Y., et al. (2020b). Effects of temperature and strain rate on plastic deformation mechanisms of nanocrystalline high-entropy alloys. *Intermetallics* 120, 106741. doi:10.1016/j.intermet.2020.106741

Li, L., Peng, J., Tang, S., Fang, Q., and Wei, Y. (2024b). Micromechanism of strength and damage trade-off in second-phase reinforced alloy by strain gradient plasticity theory. *Int. J. Plasticity* 176, 103970. doi:10.1016/j.ijplas.2024.103970

Li, W., Chen, S., and Liaw, P. K. (2020c). Discovery and design of fatigue-resistant high-entropy alloys. *Screen. Mat.* 187, 68–75. doi:10.1016/j.scriptamat.2020.05.047

Lu, K., Chauhan, A., Tirunilai, A. S., Freudenberger, J., Kauffmann, A., Heilmaier, M., et al. (2021). Deformation mechanisms of CoCrFeMnNi high-entropy alloy under low-cycle-fatigue loading. *Acta Mat.* 215, 117089. doi:10.1016/j.actamat.2021.117089

Lu, Y., Shu, X., Li, Z., Long, H., Kong, D., Sun, S., et al. (2019). *In situ* investigation of synchronized dislocation array nucleation and phase transformation at mode I-II cracks of single-crystalline Mo. *J. Alloy. Compd.* 806, 283–291. doi:10.1016/j.jallcom.2019.07.254

Luo, H., Sohn, S. S., Lu, W., Li, L., Li, X., Soundararajan, C. K., et al. (2020). A strong and ductile medium-entropy alloy resists hydrogen embrittlement and corrosion. *Nat. Commun.* 11, 3081. doi:10.1038/s41467-020-16791-8

Luo, R., Wang, B., Wang, Q., Yu, J., and Gao, Z. (2024). Cyclic degradation mechanisms of Al0. 3CoCrFeNi high-entropy alloy under different loading rates. *Mat. Today Commun.* 38, 107640. doi:10.1016/j.mtcomm.2023.107640

Nene, S. S., Frank, M., Liu, K., Sinha, S., Mishra, R. S., McWilliams, B. A., et al. (2019). Corrosion-resistant high entropy alloy with high strength and ductility. *Screen. Mat.* 166, 168–172. doi:10.1016/j.scriptamat.2019.03.028

Nguyen, H.-G., Fang, T.-H., and Doan, D.-Q. (2023). Cyclic plasticity and deformation mechanism of AlCrCuFeNi high entropy alloy. *J. Alloy. Compd.* 940, 168838. doi:10.1016/j.jallcom.2023.168838

Peng, J., Li, F., Liu, B., Liu, Y., Fang, Q., Li, J., et al. (2020). Mechanical properties and deformation behavior of a refractory multiprincipal element alloy under cycle loading. *J. Micromech. Mol. Phy.* 5, 2050014. doi:10.1142/s2424913020500149

Peng, J., Li, L., Li, F., Liu, B., Zherebtsov, S., Fang, Q., et al. (2021). The predicted rate-dependent deformation behaviour and multistage strain hardening in a model heterostructured body-centered cubic high entropy alloy. *Int. J. Plast.* 145, 103073. doi:10.1016/j.ijplas.2021.103073

Picak, S., Wegener, T., Sajadifar, S. V., Sobrero, C., Richter, J., Kim, H., et al. (2021). On the low-cycle fatigue response of CoCrNiFeMn high entropy alloy with ultra-fine grain structure. *Acta Mater* 205, 116540. doi:10.1016/j.actamat.2020.116540

Plimpton, S. (1995). Fast parallel algorithms for short-range molecular dynamics. *J. Comput. Phy.* 117, 1–19. doi:10.1006/jcph.1995.1039

Shams, S. A. A., Bae, J. W., Kim, J. N., Kim, H. S., Lee, T., and Lee, C. S. (2022a). Origin of superior low-cycle fatigue resistance of an interstitial metastable high-entropy alloy. *J. Mat. Sci. Technol.* 115, 115–128. doi:10.1016/j.jmst.2021.10.010

Shams, S. A. A., Jang, G., Bae, J. W., Amanov, A., Kim, H. S., Lee, T., et al. (2022b). Low-cycle fatigue behavior and surface treatment of a twinning-induced plasticity high-entropy alloy. *Mat. Sci. Eng. A* 853, 143724. doi:10.1016/j.msea.2022.143724

Shen, Q., Kong, X., and Chen, X. (2021a). Significant transitions of microstructure and mechanical properties in additively manufactured Al–Co–Cr–Fe–Ni high-entropy alloy under heat treatment. *Mat. sci.eng. A* 815, 141257. doi:10.1016/j.msea.2021.141257

Shen, Q., Kong, X., and Chen, X. (2021b). Fabrication of bulk Al-Co-Cr-Fe-Ni high-entropy alloy using combined cable wire arc additive manufacturing (CCW-AAM): microstructure and mechanical properties. *J. Mat. Sci. Technol.* 74, 136–142. doi:10.1016/j.jmst.2020.10.037

Shimizu, F., Ogata, S., and Li, J. (2007). Theory of shear banding in metallic glasses and molecular dynamics calculations. *Mat. Trans.* 48, 2923–2927. doi:10.2320/matertrans.mj200769

Stukowski, A. (2009). Visualization and analysis of atomistic simulation data with OVITO–the Open Visualization Tool. *Model. Simul. Mat. SC.* 18, 015012. doi:10.1088/0965-0393/18/1/015012

Stukowski, A., Bulatov, V. V., and Arsenlis, A. (2012). Automated identification and indexing of dislocations in crystal interfaces. *Model. Simul. Mat. Sc.* 20, 085007. doi:10.1088/0965-0393/20/8/085007

Suzuki, K., Koyama, M., Hamada, S., Tsuzaki, K., and Noguchi, H. (2020). Planar slip-driven fatigue crack initiation and propagation in an equiatomic CrMnFeCoNi high-entropy alloy. *Int. J. Fatigue* 133, 105418. doi:10.1016/j.ijfatigue.2019.105418

Tang, Z., Yuan, T., Tsai, C.-W., Yeh, J.-W., Lundin, C. D., and Liaw, P. K. (2015). Fatigue behavior of a wrought Al0. 5CoCrCuFeNi two-phase high-entropy alloy. *Acta Mater* 99, 247–258. doi:10.1016/j.actamat.2015.07.004

Tucker, G. J., Tiwari, S., Zimmerman, J. A., and McDowell, D. L. (2012). Investigating the deformation of nanocrystalline copper with microscale kinematic metrics and molecular dynamics. *J. Mecha. Phy. Solids* 60, 471–486. doi:10.1016/j.jmps.2011.11.007

Wang, H., Lin, Z., Qin, B., Sun, J., Su, F., Liang, Z., et al. (2024). High-temperature wear resistance improvement mechanism of TiAlCrNiSiNbx high-entropy alloy films through sliding wear-induced gradient nanostructure. *Tribol. Int.* 196, 109725. doi:10.1016/j.triboint.2024.109725

Wang, R., Tang, Y., Li, S., Zhang, H., Ye, Y., Ai, Y., et al. (2019). Novel metastable engineering in single-phase high-entropy alloy. *Mat. Des.* 162, 256–262. doi:10.1016/j.matdes.2018.11.052

Wang, X., Bai, W., Zhang, Z., Wang, Z., and Ren, X. (2023a). Enhanced fatigue resistance of a face-centered-cubic single-phase Al0. 3CoCrFeNi high-entropy alloy through planar deformation characteristic. *Mat. Sci. Eng. A* 862, 144499. doi:10.1016/j.msea.2022.144499

Wang, Y., Tan, F., Li, J., Liu, B., and Fang, Q. (2023b). Unrevealing grain boundary mobility in the precipitate hardening high entropy alloys. *J. Alloy. Compd.* 960, 170952. doi:10.1016/j.jallcom.2023.170952

Yan, J., Yin, S., Asta, M., Ritchie, R. O., Ding, J., and Yu, Q. (2022). Anomalous size effect on yield strength enabled by compositional heterogeneity in high-entropy alloy nanoparticles. *Nat. Commun.* 13, 2789. doi:10.1038/s41467-022-30524-z

Yang, W., Luo, J., Fu, H., Cheung, C. F., Ruan, H., and Yang, X.-S. (2022). bcc→ hcp phase transition significantly enhancing the wear resistance of metastable refractory high-entropy alloy. *Screen. Mat.* 221, 114966. doi:10.1016/j.scriptamat.2022.114966

Yin, S., Zuo, Y., Abu-Odeh, A., Zheng, H., Li, X.-G., Ding, J., et al. (2021). Atomistic simulations of dislocation mobility in refractory high-entropy alloys and the effect of chemical short-range order. *Nat. Commun.* 12, 4873. doi:10.1038/s41467-021-25134-0

Zhang, J., Zhang, M., Deng, L., Jin, J., Gong, P., Tang, X., et al. (2024). Probing phase transformation and dislocation evolution in high-entropy alloy under cyclic loadings. *Mat. Lett.* 136940. doi:10.1016/j.matlet.2024.136940

Zhang, L., Xin, H., Zhao, D., Li, Z., and Ma, S. (2022). Effect of twin boundary density on mechanical behavior of Al0. 1CoCrFeNi high-entropy alloy by molecular dynamics simulation. *Front. Mat.* 9, 849051. doi:10.3389/fmats.2022.849051

Zou, J.-P., Luo, X.-M., Zhang, B., Luo, Y.-W., Chen, H.-L., Liang, F., et al. (2022). Enhancing bending fatigue resistance of the CoCrFeMnNi high-entropy alloy thin foils by Al addition. *Mat. Sci. Eng. A* 831, 142281. doi:10.1016/j.msea.2021.142281